Oxidation of tetracycline and oxytetracycline for the photo-Fenton process: their transformation products and toxicity assessment

Chee-Hun Han[a,b], Hee-Deung Park[b,c], Song-Bae Kim[d,e], Viviane Yargeau[f], Jae-Woo Choi[a], Sang-Hyup Lee[a,b*], Jeong-Ann Park[e,f*]

[a] *Center for Water Resource Cycle Research, Korea Institute of Science and Technology, Hwarangno 14-gil 5, Seongbuk-gu, Seoul 02792, Republic of Korea*

[b] *KU-KIST Green School, Graduate School of Energy and Environment, Korea University, 145 Anam-ro, Seongbuk-gu, Seoul 02841, Republic of Korea*

[c] *School of Civil, Environmental and Architectural Engineering, Korea University, Anam-ro 145, Seongbuk-gu, Seoul 02841, Republic of Korea*

[d] *Environmental Functional Materials and Water Treatment Laboratory, Department of Rural Systems Engineering, Seoul National University, Seoul 08826, Republic of Korea*

[e] *Research Institute of Agriculture and Life Sciences, Seoul National University, Seoul 08826, Republic of Korea*

[f] *Department of Chemical Engineering, McGill University, 3610 University St., Montréal, H3A 0C5 Québec, Canada*

*Corresponding authors. Jeong-Ann Park, E-mail: pjaan720@snu.ac.kr and

Sang-Hyup Lee, E-mail: yisanghyup@kist.re.kr

These corresponding authors contributed equally.

Abstract

Advanced oxidation processes have gained significant attention as tetracycline (TC) and oxytetracycline (OTC) treatment, however, their oxidation using the photo-Fenton process has not been sufficiently studied. Although degradations of TC and OTC were enhanced by increasing H_2O_2 and Fe^{2+} within the ranges (H_2O_2 = 20 – 50 mg/L and Fe = 1 –10 mg/L) under UV irradiation, the further photo-Fenton process were conducted with the concentrations of 20 mg/L of H_2O_2 and 5 mg/L of Fe^{2+} to consider cost-effectiveness. Various oxidation processes including H_2O_2, ultraviolet (UV), UV/H_2O_2, and UV/H_2O_2/Fe^{2+} (photo-Fenton) for the TC and OTC degradation were compared; in conclusion, the photo-Fenton process was the most effective to remove them. The inhibition effects of several inorganic anions on the degradation of TC and OTC using the photo-Fenton process were decreased as follows: HPO_4^{2-} > HCO_3^- >> SO_4^{2-} > Cl^-. The TC and OTC degradation are generally improved by increasing pH, which is opposite to the $k_{pCBA,obs}$ values, caused by increasing the deprotonation degree of TC and OTC. A total of four and nine transformation products of TC and OTC, respectively, were detected. Among the transformation products, m/z 443.14 ($C_{22}H_{22}N_2O_8$) obtained during TC degradation, and m/z 433.16 ($C_{20}H_{20}N_2O_9$) and m/z 415.15 ($C_{20}H_{18}N_2O_8$) obtained during OTC degradation were newly observed. *Vibrio fischeri* toxicity assessment indicated that the inhibition ratio was effectively decreased by decreasing TC concentration, while, OTC was transformed into a more toxic by-product (m/z 477.15b), which was identified using the quantitative structure activity relationship (QSAR). This toxic by-product caused higher inhibition ratios than those of parental compound (OTC), and then, further oxidized as the photo-Fenton process proceeded, decreasing the inhibition ratios.

Keywords: photo-Fenton process; (oxy)tetracycline; water quality parameters; transformation products; toxicity assessment; QSAR analysis

1. Introduction

Antibiotics are one of the largest groups of pharmaceutical substances used worldwide for treating diseases in humans as well as for preventing diseases and promoting growth in livestock (Jeong et al., 2010). Tetracycline antibiotics (TCs) have received significant interest because they are broad-spectrum antibiotics against both gram-positive and gram-negative bacteria and have extensively used as antibacterial agents and veterinary medicine (Ge et al., 2018; Yamal-Turbay et al., 2013; Wang et al., 2011). Moreover, TCs are rarely adsorbed and most of them are excreted through urine and feces without being metabolized in the human body or livestock (Wammer et al., 2011; Sarmah et al., 2006). Therefore, concentration of TCs have been detected worldwide in surface water sources, ground waters, sediments, soils, and even drinking water sources in tens to hundreds μg L^{-1} range (Rahmah et al., 2011; Klavarioti et al., 2009). Moreover, concentration of TCs in livestock waste water is monitored as 2 mg L^{-1} (de Godos et al., 2012). The presence of TCs in water sources represents a threat to humans and ecosystems because of drug-resistant bacteria development and the toxicity of the antibiotics (Macauley et al., 2006; Pei et al., 2007). Thus, it is very important to remove TCs from contaminated water before discharging it into the environment. However, it is difficult to remove TCs using conventional water treatment processes such as physico-chemical or biological treatment due to their stable structure, tetracene ring, and their antibiotic properties against bacteria (Batt et al., 2007; Watkinson et al., 2007).

Recently, advanced oxidation processes (AOPs) have been proposed as effective treatment methods for water decontamination because they can generate hydroxyl radicals (HO•), which are non-selective oxidants and exhibit a high oxidation potential of 2.72 V (Shah et al., 2013; He et al., 2014). HO• present high second-order rate constants, in the 10^{8} – 10^{10} M^{-1} s^{-1} range (Haag et al., 1992), against organic substances and can form OH^{-} by removing an electron from

organic substances (Mirzaei et al., 2017). In photo-Fenton process, one molecule of H_2O_2 is decomposed into two molecules of HO• by UV irradiation, as shown in Eq. (1) (Baxendale et al., 1957). Also, HO• can be generated by the reaction of H_2O_2 and Fe^{2+} in Fenton process, and HO• can be additionally generated by photo-Fenton process in which oxidized Fe^{3+} is reduced to Fe^{2+} by UV irradiation (Eqs. (2) – (5)) (Kušić et al., 2006).

$$H_2O_2 + h\nu \rightarrow 2HO\bullet \quad (1)$$

$$Fe^{2+} + H_2O_2 \rightarrow Fe^{3+} + HO\bullet + OH^- \quad (2)$$

$$Fe^{3+} + H_2O_2 \rightarrow Fe^{2+} + HO_2\bullet + H^+ \quad (3)$$

$$Fe^{3+} + H_2O + h\nu \rightarrow Fe^{2+} + HO\bullet + H^+ \quad (4)$$

$$Fe^{3+} + H_2O_2 + h\nu \rightarrow Fe^{2+} + HO_2\bullet + H^+ \quad (5)$$

Despite this effective HO• generation, several studies on removing TC and OTC using the photo-Fenton process have been conducted to date using quite high concentrations of H_2O_2 (50 – 100 mg/L) and Fe^{2+} (2 – 5 mg/L) (Yamal-Turbay et al., 2013; Pereira et al., 2014; Michael et al., 2019; Huang et al., 2019; Zhu et al., 2019); because the studies are likely to focus on verifying the effect of UV (Yamal-Turbay et al., 2013) or solar irradiation (Pereira et al., 2014; Michael et al., 2019). Also, iron based heterogeneous catalysts have been widely studying so far, effectiveness on treating TCs is still controversial owing to requiring long reaction time and quite high H_2O_2 concentration (> 340 – 3400 mg/L) (Huang et al., 2019; Zhu et al., 2019). Nevertheless, there is a lack of study to apply the photo-Fenton (UV/H_2O_2/Fe^{2+}) process with low concentration of H_2O_2 and Fe^{2+}.

Meanwhile, new concerns about incomplete mineralization and detoxification upon TC and OTC has been raised when applying AOPs (Khan et al., 2010; López-peñalver et al., 2010;

Yuan et al., 2011; Gómez-Ocheco et al., 2012), thus, verifying degradation pathways of TC and OTC and evaluating toxicities of their transformation products are recently getting more attention. Especially, López-peñalver et al. (2010), Yuan et al. (2011), and Gómez-Ocheco et al. (2012) reported that inhibition of *Vibrio fischeri (V. fischeri)* increased for treating OTC and TC during the beginning of UV/H_2O_2 process. In addition, Hou et al. (2016) observed maximum *Daphnia magna* immobilization (100%) was reached after 60 min reaction of ultrasound assisted Fenton-like degradation of TC. Although many previous studies have identified transformation products of TC and OTC for H_2O_2 (Chen et al., 2017), UV/H_2O_2 (Liu et al., 2016; Yuan et al. 2011), to the best of our knowledge, there is no comprehensive study of comparing identified transformation products of TC and OTC and evaluating its possible toxicity based on both microbial toxicity assessment and quantitative structure activity relationship (QSAR) analysis for the photo-Fenton process (UV/H_2O_2/Fe^{2+}) so far. Microbial toxicity assessment is one of well-known and simple methods, however, it is difficult to determine which transformation product is more toxic than others because they were mixed. To overcome this limitation, QSAR analysis is first employed to predict ecotoxicological potential of each identified transformation products of TC and OTC through correlating molecular structure to biological toxicity.

Therefore, the objectives of this research were as follows: 1) to determine the Fenton reagent concentrations for the degradation of TC and OTC; 2) to compare the degradation of TC and OTC during the sole H_2O_2, UV, UV/H_2O_2, and photo-Fenton(UV/H_2O_2/Fe^{2+}) processes; 3) to investigate the effects of several inorganic anions (Cl^-, HCO_3^-, SO_4^{2-}, and HPO_4^{2-}) and the initial pH (3.1 – 8.5) on the degradation of TC and OTC using the photo-Fenton process, 4) to identify the transformation products of TC and OTC; and 5) to assess their toxicities using the bioluminescence of *Vibrio fischeri (V. fischeri)* and QSAR analysis.

2. Materials and Methods

2.1. Materials

Tetracycline ($C_{22}H_{24}N_2O_8$, MW: 444.43, purity > 98%) and oxytetracycline hydrochloride ($C_{22}H_{24}N_2O_9 \cdot HCl$, MW: 496.89, purity > 95%) were purchased from Sigma-Aldrich (St. Louis, MO, USA). Iron (II) chloride tetrahydrate ($FeCl_2 \cdot 4H_2O$, purity = 98%, Sigma-Aldrich, St. Louis, MO, USA) and hydrogen peroxide (H_2O_2, 32% v/v, OCI, Seoul, Korea) were used as Fenton reagents. Sodium chloride (NaCl, SHOWA, Kyodai, Japan), sodium hydrogen carbonate ($NaHCO_3$, SHOWA, Kyodai, Japan), sodium sulfate (Na_2SO_4, SHOWA, Kyodai, Japan) and sodium phosphate dibasic dehydrate ($Na_2HPO_4 \cdot 2H_2O$ Sigma-Aldrich, St. Louis, MO, USA) were used as sources of inorganic anions. The quencher for the residual H_2O_2 was sodium thiosulfate ($Na_2S_2O_3$, Sigma-Aldrich, St. Louis, MO, USA). Hydrochloride acid (HCl, WAKO, Osaka, Japan) and sodium hydroxide (NaOH, Samchun, Seoul, Korea) were used for pH adjustment. 4-Chlorobenzoic acid (pCBA, $C_7H_5ClO_2$, MW: 156.57, purity = 99%, Sigma-Aldrich, St. Louis, MO, USA) was used for analysis of generation rate of HO•. Methanol (purity > 99.9%, high-performance liquid chromatography (HPLC) grade, J.T.Baker, NJ, USA), oxalic acid solution (Samchun, Seoul, Korea) and acetonitrile (ACN, Merck KGaA, Darmstadt, Germany) were used for analyzing TC and OTC.

2.2. Analysis of TC and OTC

The concentrations of TC and OTC were measured by HPLC (Flexar, Perkin Elmer, Waltham, MA, USA) equipped with an UV detector. The wavelengths of the UV detector were set at 270 nm and 355 nm for TC and OTC, respectively. We used a ZORBAX SB-C18 (5 μm, 4.6

× 150 mm, Agilent, Santa Clara, CA, USA) column. The mobile phase consisted of ACN (20%), methanol (10%), and 0.01 M oxalic acid (70%) for TC and ACN (20%), methanol (15%), and 0.01 M oxalic acid (65%) for OTC. The sample injection volume was 20 µL and the flow rates for TC and OTC were 0.6 mL/min. The method limit of detection was 0.5 mg/L for TC and OTC.

To investigate the effect of low initial concentration (1 and 10 mg/L) of each TC and OTC during the photo-Fenton process, ultra-performance liquid chromatograph (UPLC, Agilent 1290 Infinity series, Agilent Technology, Germany) equipped with a triple-quadrupole mass spectrometer (6460 Jet Stream series, Agilent Technologies) was used. A Zorbax Eclipse Plus C_{18} column (particle size = 1.8 µm, diameter = 2.1 mm, length = 100 mm) was used with formic acid (0.1%) in DI water (A) and formic acid (0.1%) in ACN solution (B) as the mobile phase at the flow rate of 0.4 mL/min. With this analytical method, the limit of detection was 0.05 µg/L for TC and OTC.

2.3. Photochemical reactor and photo-Fenton process

The UV devices used for the photochemical experiments were equipped with five 4 W low-pressure Hg UV lamps (PURITEC HNS G5, Osram, Munich, Germany), of 254 nm wavelength. The UV fluence was calculated to be 0.84 mW/cm^2 using the KI/KIO_3 actinometer method (Rahn et al., 2003; Qiang et al., 2015). All the experiments were conducted in quadruplicate using 40 mL quartz reactor for efficient UV absorbance for 60 min. The zero time of the photo-Fenton process was defined after addition of H_2O_2 when the reactor was set under the UV. The higher initial concentrations (100 mg/L) of each TC and OTC than in real water were used in this study to clearly verify their oxidation mechanisms. The concentration of H_2O_2 was varied

from 20 to 30 and 50 mg/L for the UV/H_2O_2 process. Moreover, concentrations of 1, 2, 5, and 10 mg/L of Fe^{2+} combined with 20 mg/L of H_2O_2 were used during the photo-Fenton process at pH range of 5.5 – 5.6 to evaluate the effect of the Fenton reagent concentration on each TC and OTC degradation, respectively. The degradation kinetics of each TC and OTC were studied, however, the pseudo-first-order reaction kinetics could not be applied for calculation of reaction rate, because there were a very fast TC and OTC degradation at the beginning followed by a slow degradation. To compare the degradation of TC and OTC using various oxidation processes, the sole H_2O_2, UV, UV/H_2O_2, and photo-Fenton (UV/H_2O_2/Fe^{2+}) processes were performed with 20 mg/L of H_2O_2 and 5 mg/L of Fe^{2+} for 60 min. To analyze TC (or OTC) concentration during the sole H_2O_2, UV, UV/H_2O_2, photo-Fenton process, 1 ml of the samples were taken from the reactor during desired reaction time. Except for this, we used 40 ml of the whole samples at each reaction time for further analysis. Total organic carbon (TOC) was analyzed with TOC-L analyzer (SHIMADZU, Japan) to determine mineralization of TC and OTC. The initial TOC concentration of TC (initial conc. = 100 mg/L) -or OTC (initial conc. = 100 mg/L) were 57.68 mg/L or 57.17 mg/L, respectively. The concentration of H_2O_2 was measured for the photo-Fenton process using sodium thiosulfate titrant method with hydrogen peroxide test kit (Model HYP-1, HACH, Loveland, CO, USA). Also, the pH was measured by pH benchtop meter (Orion Star A211, Thermo Scientific, Waltham, MA, USA).

2.4. Effects of competing anions and initial solution pH.

To gain a better understanding of the effects of inorganic anions and pH on the degradation TC and OTC during the photo-Fenton process, the several inorganic anions (Cl^-, HCO_3^-, SO_4^{2-} and HPO_4^{2-}) and the different initial pH (3.1- 8.5) were used under the average UV fluence of 0.84 mW/cm^2. The sampling method was the same as the mentioned above method, and the

reaction time was 60 min. The initial concentrations of each TC and OTC were 100 mg/L to verify well with the results of competing anions and initial solution pH. We added 10 mM of each anions: Cl^-, HCO_3^-, SO_4^{2-} and HPO_4^{2-} to the water, as competing inorganic anions. To exclude the effect of pH in these experiments, initial pH of solutions were adjusted to equal to initial pH of TC (5.6 – 5.8) and OTC (4.0 – 4.5) solution, respectively. To verify the effect of the pH, initial pH was adjusted to 3.1, 4.1, 5.5, 7.5 and 8.5 using 0.1 M HCl and 0.1 M NaOH solutions. The generation rates of HO• during the photo-Fenton process were investigated at each different pH by calculating the observed rate constant of pCBA ($k_{pCBA,obs}$) (SI) using initial pCBA concentration of 20 mg/L.

2.5. Identification of the transformation products of TC and OTC

Deionized water for liquid chromatography – mass spectrometry (LC-MS grade) (Sigma-Aldrich, St. Louis, MO, USA) and TC or OTC solutions of 200 µM initial concentration were used. The transformation products of TC and OTC were analyzed using an ACQUITY UPLC™ combined with electrospray ionization and quadrupole time-of-flight mass spectrometer (UPLC/ESI-QTOF-MS, Synapt G2, waters, Milford, MA, USA) with sampling (1 – 120 min) during the photo-Fenton process (20 mg/L of H_2O_2 and 5 mg/L of Fe^{2+}). Water Acquity BEH C18 (1.7 µm, 2.1 × 100 mm, Waters, Milford, MA, USA) column was used and the temperature was set at 40 °C. The mobile phase consisted of A: 0.1% formic acid (FA) in H_2O and B: 0.1% FA in ACN, with a gradient of 3% B which was increased to 100% in 10 min, was maintained for 0.5 min, and decreased back to 3% B in the next 1.5 min. The flow rate and sample injection volume were 0.4 mL/min and 5 µL, respectively. The mass spectrometric analysis (m/z 50 – 1400) were conducted using electrospray ionization (ESI) source in positive mode with source temperature of 120 °C, desolvation temperature of 550 °C, desolvation gas flow of 900 L/h, and

capillary of 2.0 kV. Data acquisition was handled by MassLynx (v4.1) software (Waters, Milford, MA).

2.6. Toxicity assessment

The toxicities of TC, OTC, and their transformation products before and after photo-Fenton reaction were assessed by measuring the inhibition ratio of the bioluminescence of *V. fischeri*. For assessing the toxicity of *V. fischeri,* BioTox™ Watertox™ Standard Kit (EBPI, Mississauga, ON, Canada) was used. For preparing samples of TC, OTC, and their transformation products, 200 µM of either TC or OTC, 20 mg/L of H_2O_2 and 5 mg/L of Fe^{2+} were used for the photo-Fenton process. Samples were collected after 1, 5, 10, 20, 30, and 60 min of reaction time, and the pH of all samples were adjusted to pH 7.5 using 0.1 M NaOH to obtain stability of *V. fischeri*. The bioluminescence of the samples was measured after 15 min of exposure at 15 °C using a Victor3 multiple plate reader (Perkin Elmer, Waltham, MA, USA) with a 535/40 emission filter. The bioluminescence inhibition ratio (%) was calculated using Eq.(11):

$$bioluminescenceinhibitionratio = \frac{L_{blank} - L_{sample}}{L_{blank}} \times 100 \qquad (11)$$

where L_{Blank} and L_{sample} are the bioluminescence signals after 15 min of exposure for the sample without TCs and tested samples, respectively. Furthermore, QSAR analysis was conducted to assess the ecotoxicological potential of the identified TC, OTC and their transformation products from the photo-Fenton process by using the ECOSAR program of the EPIWIN software (Sui et al., 2017). The lethal concentration 50 (LC_{50}) values for fish (96 h); and daphnia (48 h), and the half maximal effective concentration (EC_{50}) for green algae (96 h) were provided.

3. Results and discussion

3.1. Effect of Fenton reagent concentration

As shown in Fig.1, each of TC and OTC was degraded by 28.3% and 13.0%, respectively, for 60 min in sole H_2O_2 process. Under UV irradiation alone, the degradation efficiencies of each TC and OTC was 6.5% and 19.2% after 60 min of direct photolysis, respectively, while 41.4% of TC and 43.5% of OTC were degraded with 20 mg/L of H_2O_2 for 60 min (Fig. 1a,b). Therefore, TC and OTC were more efficiently degraded in UV/H_2O_2 process than UV process because of HO• generated by decomposing H_2O_2 under UV irradiation. Similarly, Kim et al. (Kim et al., 2009) determined that the k values of TC increased more than 3.4 times when using UV/H_2O_2 (H_2O_2 conc. = 8.2 mg/L) than that of only UV irradiation process. During the UV/H_2O_2 process, the degradation efficiencies of each TC and OTC were increased from 41.4 to 54.7% and from 43.5 to 59.9%, respectively by increasing the H_2O_2 concentration from 20 to 50 mg/L for 60 min (Fig. 1a and Fig. 1b). In conclusion, HO• could not be effectively generated by H_2O_2 (< 50 mg/L) under UV irradiation, leading to the slight increase in the degradation rate of each TC and OTC.

To verify the effect of Fe^{2+} for the photo-Fenton process, the concentration of Fe^{2+} varied from 1 to 10 mg/L with 20 mg/L of H_2O_2 concentration. The photo-Fenton reaction generally occurs very fast at the beginning of the process because HO• is rapidly generated during the reaction of Fe^{2+} and H_2O_2 under UV irradiation (Mirzaei et al., 2017). Likewise, the degradation of each TC and OTC occurred very fast within 1 min, but slowly thereafter, then, k_{obs} could not be calculated. The highest degradation efficiencies of each TC and OTC were obtained equally as 97.1% during the photo-Fenton process when 20 mg/L of H_2O_2 and 10 mg/L of Fe^{2+} were used for 60 min (Fig. 1c,d). However, high TC and OTC degradation efficiencies were also achieved as 94.2 and 94.8%, respectively, by using 5 mg/L of Fe^{2+} which were slightly

lower than those with 10 mg/L of Fe^{2+}. In addition, a relatively large amount of iron oxides were precipitated when adding 10 mg/L of Fe^{2+} to the reaction mixture. Similarly, Karatas et al. (Karatas et al., 2012) studied the photo-Fenton process using high concentrations of Fe^{2+}, which resulted in the precipitation of Fe^{2+} and Fe^{3+} as iron hydroxide. During the photo-Fenton process with 5 mg/L of Fe^{2+}, the concentration of H_2O_2 (ini = 20 mg/L) was decreasing well to 12.5 mg/L and 3.5 mg/L for 10 and 30 min, respectively. Thus, the photo-Fenton process were conducted with the Fenton reagent concentrations of 20 mg/L of H_2O_2 and 5 mg/L of Fe^{2+} for further experiments.

3.2. Comparison of the TC and OTC degradation using various oxidation processes

The degradation efficiencies of each TC and OTC using sole H_2O_2, UV, UV/H_2O_2, and the photo-Fenton processes were compared for 30 min, as shown in Fig. 2. The degradation efficiencies of each TC and OTC using H_2O_2 for 30 min were 27.9 and 12.7%, respectively (Fig. 2a). As an oxidant, H_2O_2 partly degraded TC and OTC by its oxidation potential as 1.80 V (Chen et al., 2017). Using the UV process, 11.7% of OTC was degraded, which was 7.4% higher than the amount of TC degraded for 30 min (Fig. 2a). This result was attributed by the much high molar extinction coefficient of OTC at 254 nm (19,799 M^{-1} cm^{-1}) than that of TC (4,108 M^{-1} cm^{-1}) (Kim et al., 2009). During UV/H_2O_2 process for 30 min, the degradation efficiencies of TC and OTC were 34.2% and 34.4%, respectively. When using the photo-Fenton process, both TC and OTC were the most effectively degraded to a similar level and the degradation efficiencies of TC and OTC were 91.3% and 92.4% for 30 min, respectively. Therefore, both TC and OTC were more degraded using the photo-Fenton process than H_2O_2, UV and UV/H_2O_2 processes (Fig. 2a).

During the photo-Fenton process, 82.5% and 97.5% of H_2O_2 was consumed after 30 min and 60 min reaction (Fig. 2b). Although H_2O_2 is steadily consumed during the photo-Fenton process, the complete removal of TC and OTC were not reached because of very high initial concentration of TC and OTC (100 mg/L). About 10% of TOC mineralization were observed for 60 min of the photo-Fenton process despite high degradation efficiency of TC (94.6%) and OTC (95.0%), which indicated that TC and OTC were not completely mineralized because they transformed to recalcitrant compounds during the photo-Fenton process. Further discussion of transformation products of TC and OTC produced by the photo-Fenton process were addressed in section 3.5. In order to consider expected concentration of TC and OTC in real pharmaceutical and livestock wastewater (Li et al., 2004; de Godos et al., 2012), the initial concentrations of TC and OTC (1 and 10 mg/L) were also applied to verify the effect of initial concentrations for the photo-Fenton process (Fig. 3a,b). At initial concentration of 10 mg/L, over 90% of TC and OTC degradation were achieved after 1 min. As for initial concentration of 1 mg/L, almost completely (over 99%) of TC and OTC degradation were achieved after 5 min. Therefore, the photo-Fenton process is an effective way to remove both TC and OTC in concentration range of real contaminated water. Also, degradation efficiencies of TC and OTC were enhanced by decreasing initial concentration of TC or OTC.

3.3. Effect of inorganic anions: Cl^-, HCO_3^-, SO_4^{2-}, and HPO_4^{2-}

Inorganic anions could generally inhibit the generation of HO• during the photo-Fenton process via complexing with ferrous ion or scavenging (Hassanshahi et al., 2018). As can be seen in Fig. 3c,d, when coexisting with 10 mM of each Cl^-, SO_4^{2-}, HCO_3^-, and HPO_4^{2-}, the degradation efficiencies of TC for 60 min were 94.8, 94.8, 89.6, and 85.2%, respectively, and those of OTC were 95.2, 95.1, 75.2, and 72.1%, respectively. Relatively small inhibition effects were

observed for Cl^- and SO_4^{2-} because SO_4^{2-} has low reactivity with HO• and Cl^- can react with HO• to form $ClOH^{\bullet-}$, which can rapidly regenerate HO• near neutral pH values (Liu et al., 2016; Gao et al., 2009); thus, 10 mM of Cl^- was considered to have insignificant inhibition effects on the degradation of TC and OTC in this study. From similar studies, there were no inhibition effects on the degradation of OTC using UV/H_2O_2 (Liu et al., 2016) and solar photo-Fenton (Pereira et al., 2014) process, competing with low concentration of Cl^- (< 17 mM) and SO_4^{2-} (< 4 mM). However, HPO_4^{2-} greatly inhibited the degradation of TC and OTC, more than HCO_3^- did, because HCO_3^- could generate $CO_3^{\bullet-}$, which has an oxidation potential of 1.78 V (Cope et al., 1973), by reacting with HO•, thus, leading to the degradation of TC and OTC. Whereas, HPO_4^{2-} not only reacted as HO• scavenger, but reacted with ferrous iron to form insoluble iron phosphate complexes, which greatly inhibited the Fenton reaction (Gutiérrez-Zapata et al., 2017). Therefore, the degradation efficiencies of both TC and OTC decreased because the presence of inorganic anions generally inhibited the degradation of TC and OTC during the photo-Fenton process, since inorganic anions acted as HO• scavengers and competitors and the order of inhibition was the following: $HPO_4^{2-} > HCO_3^- >> SO_4^{2-} > Cl^-$.

3.4. Effect of initial pH

As illustrated in Fig. 4a,b, the pH range was set from 3.1 to 8.5 to investigate the influence of the initial pH on the degradation of each TC and OTC during the photo-Fenton process. The initial pH is the most important factor affecting the photo-Fenton process and the photo-Fenton reaction (HO• generation) is generally enhanced under acidic condition because high reactive Fe^{2+} ions are dominant (Jain et al., 2018). Similarly, in previous studies, the degradation efficiencies of other antibiotics, including amoxicillin (Elmolla et al., 2009), cloxacillin (Elmolla et al., 2009) and ampicillin (Elmolla et al., 2009 ; Rozas et al., 2010), were steadily increased

by decreasing pH attributed to high HO• generation. As shown in Fig. 4c, as pH decreased from 8.5 to 3.1, the $k_{pCBA,obs}$ increased from 4.17 × 10^{-4} s^{-1} to 7.27 × 10^{-4} s^{-1}. However, unlike the degradation of pCBA, the degradation of TC and OTC was inhibited at pH 3.1. Also, TC was the most degraded at pH 8.5 while the degradation of OTC was the most inhibited. It should be noted that enhancement in their degradation rate at higher pH can be affected by increasing photolysis rate at UV (λ = 254 nm) and reaction rate constant with HO• by increasing the deprotonation degree of TC and OTC, more than generated HO• amount. There are many dissociated forms of TC (TCH_3^+, TCH_2^0, TCH^-, TC^{2-}) and OTC (H_3OTC^+, H_2OTC, $HOTC^-$, OTC^{2-}) at pH range of 3.1 – 8.5, which exhibit distinct physicochemical properties. At pH 3.1, TC was protonated to be TCH_3^+, which became low reactive molecule (Mohammed-Ali, 2012) causing less susceptible to HO• attack. With the increase of pH, the degree of deprotonation increases by TCH_2^0, TCH^-, and TC^{2-}, which results in the increasing photolysis rate. Ge et al. found that TC^{2-} is the fastest degradable form for the photolysis followed by TCH^- and TCH_2^0 (Ge et al., 2018). Moreover, TCH^- (105.78 × 10^9 M^{-1} s^{-1}) and TC_2^- (35.29 × 10^9 M^{-1} s^{-1}) are highly reactive toward HO• than TCH_2^0 (6.37 × 10^9 M^{-1} s^{-1}) (Ge et al., 2018). Similarly, UV photolysis of OTC was the highest when deprotonated as OTC^{2-} followed by $HOTC^-$, H_2OTC, and H_3OTC^+ under pH 3 - 11 by the increasing molar absorptivity at 254 nm (Liu et al., 2015). Also, the reactivity toward HO• is higher in the order: OTC^{2-} > $HOTC^-$ > H_2OTC > H_3OTC^+ (Liu et al., 2015). In spite of strong HO• scavengers, such as hydroxide anion (OH^-) and hydroperoxide anion (HO_2^-), are majorly present (Buxton et al., 1988; Christensen et al., 1982), the highest degradation of TC was achieved at pH 8.5 due to the most highly reactive TCH^-; however, degradation of OTC was significantly inhibited at the beginning of the reaction by the fact that the relatively slight increase of HO• reactivity among OTC dissociated forms might not fully overcome competing effect toward HO•. As a results, although the pseudo-first rate constant values of pCBA were

about 57.4% decreasing by increasing pH from 3.1 to 8.5, deprotonated TC (TCH^-) and OTC (H_2OTC and $HOTC^-$) can enhance their degradation efficiencies via highly photolysis and reactive toward HO•. Therefore, pH 5.5 might be effective to degrade TC and OTC using the photo-Fenton process.

3.5. Identification of transformation products of TC and OTC

The transformation products of TC (m/z 461.15, 459.14, 443.14, and 413.13) and OTC (m/z 477.15 (two products), 475.14, 459.14, 449.15, 447.14, 433.16a,b (two products), and 415.15) were identified for the photo-Fenton process (Table S1). As indicated in Fig. 5a, the m/z 461.15 transformation product from the degradation of TC was assumed to be the primary transformation product at the beginning of the photo-Fenton process, since the C11a–C12 double-bond of TC was a susceptible site for the HO• attack. Wang et al. (2011) also found that m/z 461 was attacked by free ozone or HO• during the ozonation of TC. Furthermore, the dehydration of C6–C5a were first observed (m/z 443.14) in this study, which belongs to the leading stable aromatic ring. The molar mass of the m/z 459.15 transformation product was 14 Da higher than that of the parent TC. This is attributed to the formation of an aldehyde group (HC=O). Also, the m/z 413.13 transformation product was formed by the dehydration of C6–C5a and demethylation. The transformation products of OTC were more varied than those of TC included hydroxylation, decarbonylation, demethylation, secondary alcohol oxidation, and dehydaration (Fig. 5b). The hydroxylation products (m/z 477.15) were generated by adding hydroxyl groups to the aromatic ring (m/z 477.15a) and C11a–C12 double-bond of OTC (m/z 477.15b). Hydrogen abstraction at C5 formed the m/z 459.14 product, and m/z 475.14 was formed by combining hydroxyl addition to the aromatic ring with hydrogen abstraction. The m/z 433.16a transformation product was engaged in a loss of CO at C1, then m/z 449.15 was formed by further

hydroxyl addition to aromatic ring. Demethylation was involved in the abstraction of one methyl group (m/z 447.14) and two methyl groups (m/z 433.16b) of dimethylammonium group at C4. Also, dehydration at C3 generated m/z 415.15. Similarly, Liu et al. (2016) reported five degradation pathways for OTC using the UV/H_2O_2 process and same seven transformation products (m/z 477.15 (two products), 475.14, 459.14, 449.15, 447.14, and 433.16) were observed in this study. However, the m/z 433.16 ($C_{20}H_{20}N_2O_9$) and 415.15 ($C_{20}H_{18}N_2O_8$) transformation products were newly observed during the photo-Fenton process.

3.6 Toxicity of TC and OTC transformation products

The $EC_{50,\ 15min}$ of TC and OTC against *V. fischeri* were calculated to be 104 μM (Tong et al., 2015) and 152 μM (Yuan et al., 2011) when 200 μM of TC and OTC were used as the initial concentration during toxicity assessments. The toxicities for *V. fischeri* of TC, OTC, and their transformation products were investigated during the photo-Fenton process (Fig. 6). The inhibition ratio of TC was the highest: 62.83% for the control sample (TC = 200 μM), then gradually decreased by increasing the reaction time of the photo-Fenton process (Fig. 6a). This result indicated that the toxicity for *V. fischeri* was attributed to the decreasing TC concentration and the transformation products of TC becoming less toxic than TC itself. After 60 min of the photo-Fenton process, the inhibition ratio of TC and its transformation products for *V. fischeri* was 13.72 %. On the other hand, the inhibition ratio of OTC (200 μM) for *V. fischeri* was estimated to be 42.85%. However, the inhibition ratios of OTC and its transformation by-products were higher than 90% during the photo-Fenton process (1 – 30 min) although OTC concentration steadily decreased (Fig. 6b). This meant that OTC was transformed into be more toxic compound for *V. fischeri* during the photo-Fenton reaction even after very short reaction time (1 min). Table 1 shows the predicted toxicity values of OTC and several transformation

products (m/z 415.15, 459.14, 475.14, and 477.15b), which were detected in all samples, by assessing of *V. fischeri* using the ECOSAR program. Three transformation products (m/z 415.15, 459.14, and 475.14) presented significantly lower acute toxicity for all fish, daphnia, and green algae, while m/z 477.15b exhibited significantly higher acute toxicity for fish and green algae than OTC. As a result, *V. fischeri* toxicity was decreased after 60 min as the amount of m/z 477.15b product greatly decreased (Fig. 6c). Similarly, Wang et al. (Wang et al., 2018) reported that *V. fischeri* inhibition was the highest at 10 min (55%) for electrochemical oxidation over a Ti/Ti_4O_7 anode due to more toxic transformation products with m/z 461, 432, and 477, examined by QSAR analysis. Although a high OTC concentration (200 μM) was used for toxicity assessments that would not be efficiently detoxified during photo-Fenton process. However, these results suggested that treating OTC should be more carefully considered than TC when using the photo-Fenton process and sufficient time would be required to degrade toxic transformation products into non-toxic products.

4. Conclusions

In this study, the degradation mechanism of TC and OTC using the photo-Fenton process was fully investigated, including the effects of Fenton reagent concentrations, anions, and pH; moreover, transformation products of TC and OTC were identified and evaluated their toxicity though *V. fischeri* inhibition and QSAR analysis. The degradation efficiencies of each TC and OTC was increased by increasing Fe^{2+} and H_2O_2 concentrations within the applied ranges in this study. Moreover, OTC is more sensitive to UV irradiation than TC, while the degradation of TC by HO• is higher than that of OTC. The photo-Fenton process was the most effective way to remove TC and OTC among other sole H_2O_2, UV, UV/H_2O_2 and Fenton process with short reaction time. There is a little impact on the degradation of TC and OTC with a Cl^- or

SO_4^{2-} anions at pH 5.5. A few of transformation products of TC and OTC during photo-Fenton process were newly identified in this study, and all observed transformation products of TC exhibited lower *V. fischeri* toxicity than that of TC. However, OTC could transform into a more toxic by-product to *V. fischeri* at the beginning of the photo-Fenton process, then further oxidized to non-toxic by-product with sufficient time. Therefore, without pH adjustment, the photo-Fenton process could be effective to remove TC and might be efficiently treat OTC as long as the process is operated until possibly produced toxic by-products of OTC are totally detoxified.

Acknowledgement

This research was supported by the Korea Ministry of Environment (MOE) as a Public Technology Program based on Environmental Policy (E416-00020-0606-0)

References

Batt, A.L., Kim, S., Aga, D.S., 2007. Comparison of the occurrence of antibiotics in four full-scale wastewater treatment plants with varying designs and operations. Chemosphere 68, 428-435.

Baxendale, J.H., Wilson, J.A., 1957. The photolysis of hydrogen peroxide at high light intensities. Trans. Faraday Soc. 53, 344-356.

Buxton, G.V., Greenstock, C.L., Gelman, W.P., Ross, A.B., 1988. Critical review of rate constant for reactions of hydrated electrons, hydrogen atoms and hydroxyl radicals (•OH/•O-) in aqueous solution. J. Phys. Chem. Ref. Data. 17, 513.

Chen, Y.Y., Ma, Y.L., Yang, J., Wang, L.Q., Lv, J.M., Ren, C.J., 2017. Aqueous tetracycline degradation by H_2O_2 alone: Removal and transformation pathway. Chem. Eng. J. 307, 15-23.

Christensen, H., Sehested, K., Corfitzen, H., 1982. Reactions of hydroxyl radicals with hydrogen peroxide at ambient and elevated temperatures. J. Phys. Chem. 86, 1588-1590.

Cope, V.W., Chen, S.-N., Hoffman, M.Z., 1973. Intermediates on the photochemistry of carbonato-amine complexes of cobalt(Ⅲ). CO_3^- radicals and the aquocarbonato complex. J. Am. Chem. Soc. 95, 3116-3121.

de Godos, I., Muñoz, R., Guieysse, B., 2012. Tetracycline removal during wastewater treatment in high-rate algal ponds. J. Hazard. Mater. 229, 446-449.

Elmolla, E.S., Chaudhuri, M., 2009. Degradation of the antibiotics amoxicillin, ampicillin and cloxacillin in aqueous solution by the photo-Fenton process. J. Hazard. Mater. 172, 1476-1481.

Gao, N., Deng, T., Zhao, D., 2009. Ametryn degradation in the ultraviolet (UV) irradiation/hydrogen peroxide (H_2O_2) treatment. J. Hazard. Mater. 164, 640-645.

Ge, L., Dong, Q., Halsall, C., Chen, C.E.L., Li, J., Wang, D., Zhang, P., Yao, Z., 2018. Aqueous multivariate phototransformation kinetics of dissociated tetracycline: implications for the photochemical fate in surface waters. Environ. Sci. Pollut. Res. 25, 15726-15732.

Gómez-Pacheco, C.V., Sánchez-Polo, M., Rivera-Utrilla, J., López-penalver, J.J., 2012. Tetracycline degradation in aqueous phase by ultraviolet radiation. Chem. Eng. J. 187, 89-95.

Gutiérrez-Zapata, H.M., Rojas, K.L., Sanabria, J., Rengifo-Herrera, J.A., 2017. 2,4-D abatement from groundwater sample by photo-Fenton processes at circumneutral pH using naturally iron present. Effect of inorganic ions. Environ. Sci. Pollut. Res. 24, 6213-6221.

Haag, W.R., Yao, C.C.D., 1992. Rate constants for reaction of hydroxyl radicals with several drinking water contaminants. Environ. Sci. Technol. 26, 1005-1013.

Khan, M.H., Bae, H., Jung, J.Y., 2010. Tetracycline degradation by ozonation in the aqueous phase: Proposed degradation intermediates and pathway. J. Hazard. Mater. 181, 659-665.

Hassanshahi, N., Karimi-Jashni, A., 2018. Comparison of photo-Fenton, O_3/H_2O_2/UV and photocatalytic processes for the treatment of gray water. Ecotoxicol. Environ. Saf. 161, 683-690.

He, X., Mezyk, S.P., Michael, I., Fatta-Kassinos, D., Dionysiou, D.D., 2014. Degradation kinetics and mechanism of β-lactam antibiotics by the activation of H_2O_2 and $Na_2S_2O_8$ under UV-254 nm irradiation. J. Hazard. Mater. 279, 375-383.

Hou, L., Wang, L., Royer, S., Zhang, H., 2016. Ultrasound-assisted heterogeneous Fenton-like degradation of tetracycline over a magnetite catalyst. J. Hazard. Mater. 302, 458-467.

Jain, B., Singh, A.K., Kim, H., Lichfouse, E., Sharma, V.K., 2018. Treatment of organic pollutants by homogeneous and heterogeneous Fenton reaction processes. Environ. Chem. Lett. 16, 947-967.

Jeong, J., Song, W., Cooper, W.J., Jung, J., Greaves, J., 2010. Degradation of tetracycline antibiotics: Mechanisms and kinetic studies for advanced oxidation/reduction processes. Chemosphere 78, 533-540.

Karatas, M., Argun, Y.A., Argun, M.E., 2012. Decolorization of antraquinonic dye, Reactive Blue 114 from synthetic wastewater by Fenton process: Kinetics and thermodynamics. J. Ind. Eng. Chem. 18, 1058-1062.

Kim, I., Yamashita, N., Tanaka, H., 2009. Photodegradation of pharmaceuticals and personal care products during UV and UV/H_2O_2 treatments. Chemosphere 77, 518-525.

Klavarioti, M., Mantzavinos, D., Kassinos, D., 2009. Removal of residual pharmaceuticals from aqueous systems by advanced oxidation processes. Environ. Int. 35, 402-417.

Kušić, H., Koprivanac, N., Božić, A.L., Selanec, I., 2006. Photo-assisted Fenton type processes for the degradation of phenol: A kinetic study. J. Hazard. Mater. B 136, 632-344.

Lai, C., Huang, F., Zeng, G., Huang, D., Qin, L., Cheng, M., Zhang, C., Li, B., Yi, H., Liu, S., Li, L., Chen, L., 2019. Fabrication of novel magnetic $MnFe_2O_4$/bio-char composite and heterogeneous photo-Fenton degradation of tetracycline in near neutral pH. Chemosphere 224, 910-921.

Li, S.Z., Li, X.Y., Wang, D.Z., 2004. Membrane (RO-UF) filtration for antibiotic wastewater treatment and recovery of antibiotics. Sep. Purif. Tchnol. 34, 109-114.

Liu, Y., He, X., Duan, X., Fu, Y., Dionysiou, D.D., 2015. Photochemical degradation of oxytetracycline: Influence of pH and role of carbonate radical. Chem. Eng. J. 276, 113-121.

Liu, Y., He, X., Fu, Y., Dionysiou, D.D., 2016. Degradation kinetics and mechanism of oxytetracycline by hydroxyl radical-based advanced oxidation processes. Chem. Eng. J. 284, 1317-1327.

López-peñalver, J.J., Sánchez-polo, M., Gómez-Pacheco, C.V., Rivera-Utrilla, J., 2010. Photodegradation of tetracyclines in aqueous solution by using UV and UV/H_2O_2 oxidation processes. J. Chem. Technol. Biotechnol. 85, 1325-1333.

Macauley, J.J., Qiang, J., Adams, C.D., Surampalli, R., Mormile, M.R., 2006. Disinfection of swine wastewater using chlorine, ultraviolet light and ozone. Water. Res. 40, 2017-2026.

Michael, S.G., Michael-Kordatou, I., Beretsou, V.G., Jäger, T., Michael, C., Schwartz, T., Fatta-Kassinos, D., 2019. Solar photo-Fenton oxidation followed by adsorption on activated carbon for the minimization of antibiotic resistance determinants and toxicity present in urban wastewater. Appl. Catal. B 244, 871-880.

Mirzaei, A., Chen, Z., Haghighat, F., Yerishalmi, L., 2017. Removal of pharmaceuticals from water by homo/heterogonous Fenton-type processes - A review. Chemosphere 174, 665-688.

Mohammed-Ali, M.A.J., 2012. Stability study of tetracycline drug in acidic and alkaline solutions by colorimetric method. J. Chem. Pharm. Res. 4 (2), 1319-1326.

Pei, R., Cha, J., Carlson, K.H., Pruden, A., 2007. Response of antibiotic resistance genes (ARG) to biological treatment in dairy lagoon water. Environ. Sci. Technol. 41, 5108-5113.

Pereira, J.H.O.S., Queirós, D.B., Reis, A.C., Nunes, O.C., Borges, M.T., Boaventura, R.A.R., Vilar, V.J.P., 2014. Process enhancement at near neutral pH of a homogeneous photo-Fenton reaction using ferricarboxylate complexes: Application to oxytetracycline degradation. Chem. Eng. J. 253, 217-228.

Qiang, Z., Li, W., Li, M., Bolton, J.R., Qu, J., 2015. Inspection of feasible calibration conditions for UV radiometer detectors with the KI/KIO_3 actinometer. Photochem. Photobiol. 91, 68-73.

Rahmah, A.U., Harimurti, S., Omar, A.A., Murugesan, T., 2011. Photochemical degradation of oxytetracycline hydrochloride in the presence of H_2O_2. National Postgraduate Conference, 1-4.

Rahn, R.O., Stefan, M.I., Bolton, J.R., Goren, E., Shaw, P.S., Lykke, K.R., 2003. Quantum yield of the iodide–iodate chemical actinometer: dependence on wavelength and concentration. Photochem. Photobiol. 78 (2), 146-152.

Rozas, O., Contreras, D., Mondaca, M.A., Pérez-Moya, M., Mansilla, H.D., 2010. Experimental design of Fenton and photo-Fenton reactions for the treatment of ampicillin solutions. J. Hazard. Mater. 177, 1025-1030.

Sarmah, A.K., Meyer, M.T., Boxall, A.B.A., 2006. A global perspective on the use, sales, exposure pathways, occurrence, fate and effects of veterinary antibiotics (VAs) in the environment. Chemosphere 65, 725-759.

Shah, N.S., He, X., Khan, H.M., Khan, J.A., O'Shea, K.E., Boccelli, D.L., Dionysiou, D.D., 2013. Efficient removal of endosulfan from aqueous solution by UV-C/peroxides: A comparative study. J. Hazard. Mater. 263, 584-592.

Sui, Q., Gebhardt, W., Schröder, H.F., Zhao, W., Lu, S., Yu, G., 2017. Identification of new oxidation products of bezafibrate for better understanding of its toxicity evolution and oxidation mechanisms during ozonation. Environ. Sci. Technol. 51, 2262-2270.

Tong, F., Zhao. Y., Gu, X., Gu, C., Lee, C.C.C., 2015, Joint toxicity of tetracycline with copper(II) and cadmium(II) to *Vibrio fisheri*: effect of complexation reaction. Ecotoxicology 24, 346-355.

Wammer, K.H., Slattery, M.T., Stemig, A.M., Ditty, J.L., 2011. Tetracycline photolysis in natural waters: Loss of antibacterial activity. Chemosphere 85, 1505-1510.

Wang, J., Zhi, D., Zhou, H., He, X., Zhang, D., 2018. Evaluating tetracycline degradation pathway and intermediate toxicity during the electrochemical oxidation over a Ti/Ti_4O_7 anode. Water Res. 137, 324-334.

Wang, P., He, Y.L., Huang, C.H., 2011. Reactions of tetracycline antibiotics with chlorine dioxide and free chlorine. Water. Res. 45, 1838-1846.

Wang, T., Zhang, H., Zhang, J., Lu, C., Huang, Q., Wu, J., Liu, F., 2011. Degradation of tetracycline in aqueous media by ozonation in an internal loop-lift reactor. J. Hazard. Mater. 192, 35-43.

Watkinson, A.J., Murby, E.J., Costanzo, S.D., 2007. Removal of antibiotics in conventional and advanced wastewater treatment: Implications for environmental discharge and wastewater recycling. Water. Res. 41, 4164-4176.

Yamal-Turbay, E., Jaén, E., Graells, M., Pérez-Moya, M., 2013. Enhanced photo-Fenton process for tetracycline degradation using efficient hydrogen peroxide dosage. J. Photochem. Photobiol. A Chem. 267, 11-16.

Yuan, F., Hu, C., Hu, X., Wei, D., Chen, Y., Qu, J., 2011. Photodegradation and toxicity changes of antibiotics in UV and UV/H_2O_2 process. J. Hazard. Mater. 185, 1256-1263.

Zhu, G., Yu, X., Xie, F., Feng, W., 2019. Ultraviolet light assisted heterogeneous Fenton degradation of tetracycline based on polyhedral Fe3O4 nanoparticles with exposed high-energy {110} facets. Appl. Surf. Sci. 485, 496-505.

Figure Captions

Figure 1. Degradation efficiencies of UV, UV/H_2O_2 ([H_2O_2] = 20 – 50 mg/L), and sole H_2O_2 (inset) processes for (a) TC and (b) OTC; and the photo-Fenton process ([H_2O_2] = 20 mg/L, [Fe^{2+}] = 1 – 10 mg/L) for (c) TC and (d) OTC. The error bars represent the standard deviation of the mean (n = 4).

Figure 2. (a) Comparison of degradation efficiencies of each TC and OTC using H_2O_2 ([H_2O_2] = 20 mg/L), UV (UV dose = 0.84 mW/cm^2), UV/H_2O_2 (UV dose = 0.84 mW/cm^2, ([H_2O_2] = 20 mg/L), and the photo-Fenton processes (UV dose = 0.84 mW/cm, [H_2O_2] = 20 mg/L, [Fe^{2+}] = 5 mg/L) for 30 min; (b) TOC mineralization and H_2O_2 consumption during the photo-Fenton processes. The error bars represent the standard deviation of the mean (n = 4).

Figure 3. Effects of initial concentration of (a) TC (1, 10, and 100 mg/L) and (b) OTC (1, 10, and 100 mg/L); and inorganic anions on the degradation of (c) TC (initial conc. = 100 mg/L) and (d) OTC (initial conc. = 100 mg/L) by photo-Fenton process ([Cl^-] = [HCO_3^-] = [SO_4^{2-}] = [HPO_4^{2-}] = 10 mM). The error bars represent the standard deviation of the mean (n = 4).

Figure 4. The effects of pH (pH values: 3.1 – 8.5) on the degradation of (a) TC, (b) OTC, and (c) pCBA (inset = distribution at different pH values) using the photo-Fenton process. The error bars represent the standard deviation of the mean (n = 4).

Figure 5. Degradation pathways of (a) TC and (b) OTC during the photo-Fenton process.

Figure 6. Inhibition ratio of *V. fischeri* under initial (a) TC and (b) OTC concentation of 200 μM at each photo-Fenton reaction time (0 – 60 min and 0 – 120 min, respectively). The error bars represent the standard deviation of the mean (n = 5). (c) Peak areas of four OTC transformation products (m/z 415.15, 459.14, 475.14, and 477.15b) during the photo-Fenton process for 120 min.

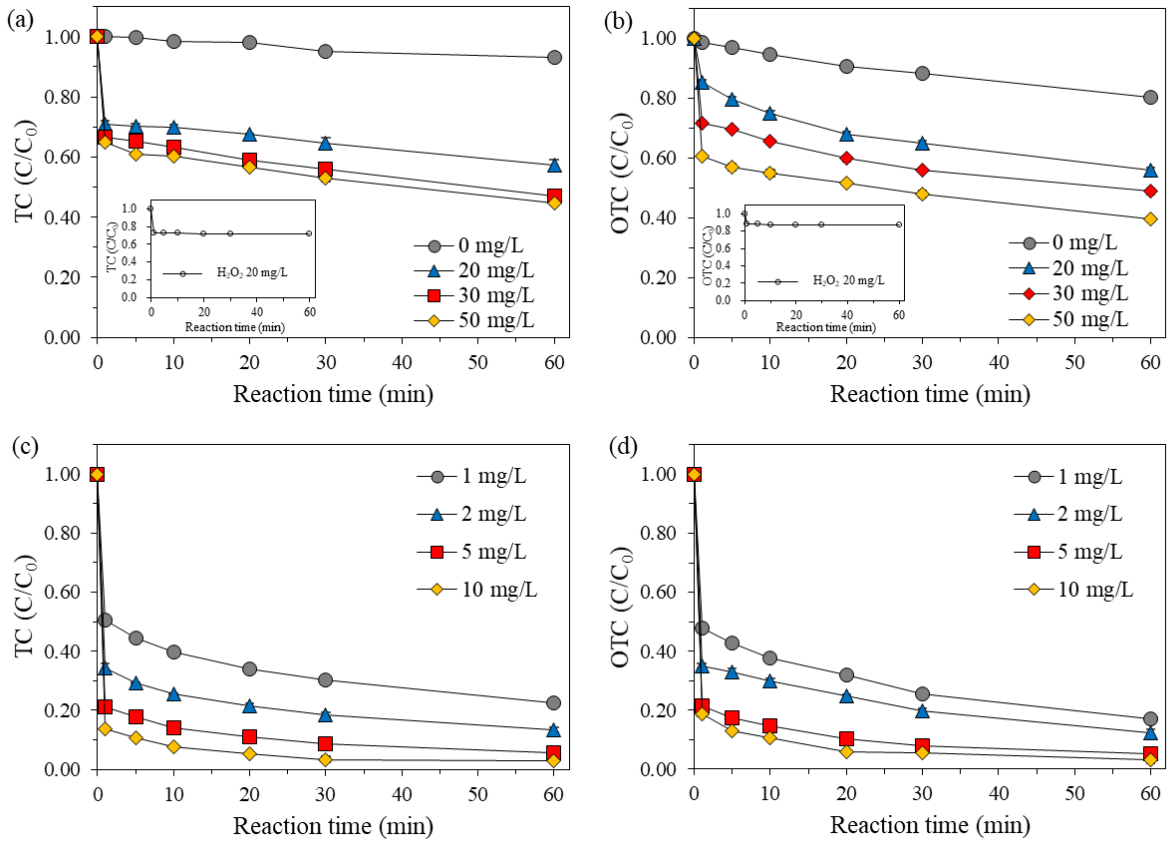
(a)
TC (C/C0)
Reaction time (min)
0 mg/L
20 mg/L
30 mg/L
50 mg/L
H2O2 20 mg/L
(b)
OTC (C/C0)
Reaction time (min)
0 mg/L
20 mg/L
30 mg/L
50 mg/L
H2O2 20 mg/L
(c)
TC (C/C0)
Reaction time (min)
1 mg/L
2 mg/L
5 mg/L
10 mg/L
(d)
OTC (C/C0)
Reaction time (min)
1 mg/L
2 mg/L
5 mg/L
10 mg/L

Fig. 1

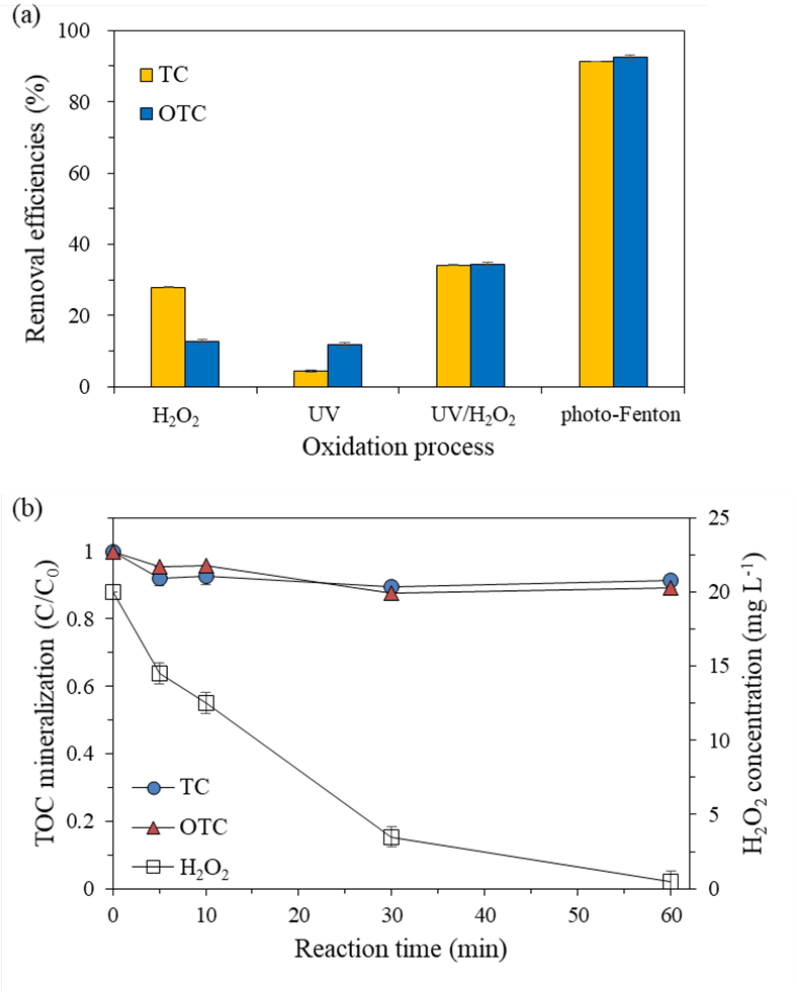
(a)
Removal efficiencies (%)
TC
OTC
H_2O_2
UV
UV/H_2O_2
photo-Fenton
Oxidation process
(b)
TOC mineralization (C/C_0)
H_2O_2 concentration (mg L^{-1})
TC
OTC
H_2O_2
Reaction time (min)

Fig. 2

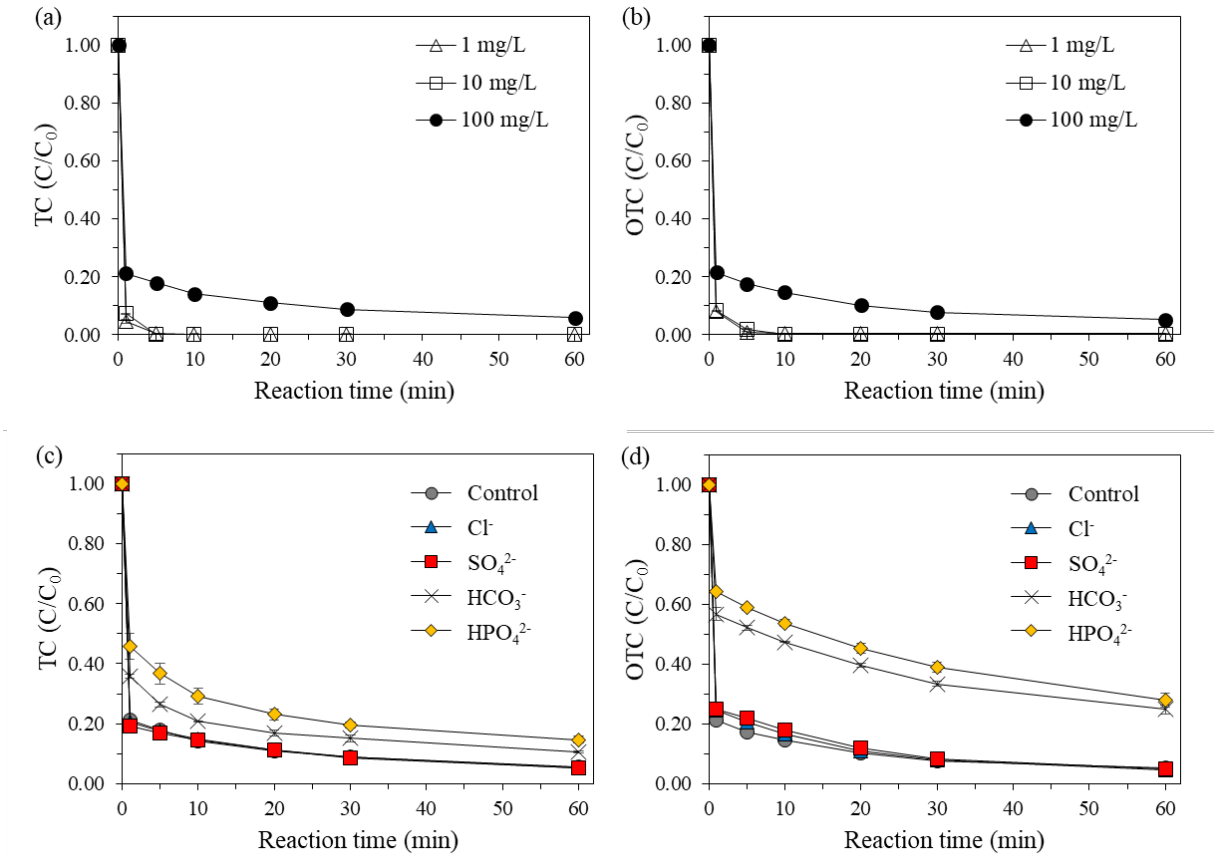
(a)
TC (C/C0)
1 mg/L
10 mg/L
100 mg/L
Reaction time (min)
(b)
OTC (C/C0)
1 mg/L
10 mg/L
100 mg/L
Reaction time (min)
(c)
TC (C/C0)
Control
Cl-
SO4 2-
HCO3-
HPO4 2-
Reaction time (min)
(d)
OTC (C/C0)
Control
Cl-
SO4 2-
HCO3-
HPO4 2-
Reaction time (min)

Fig. 3

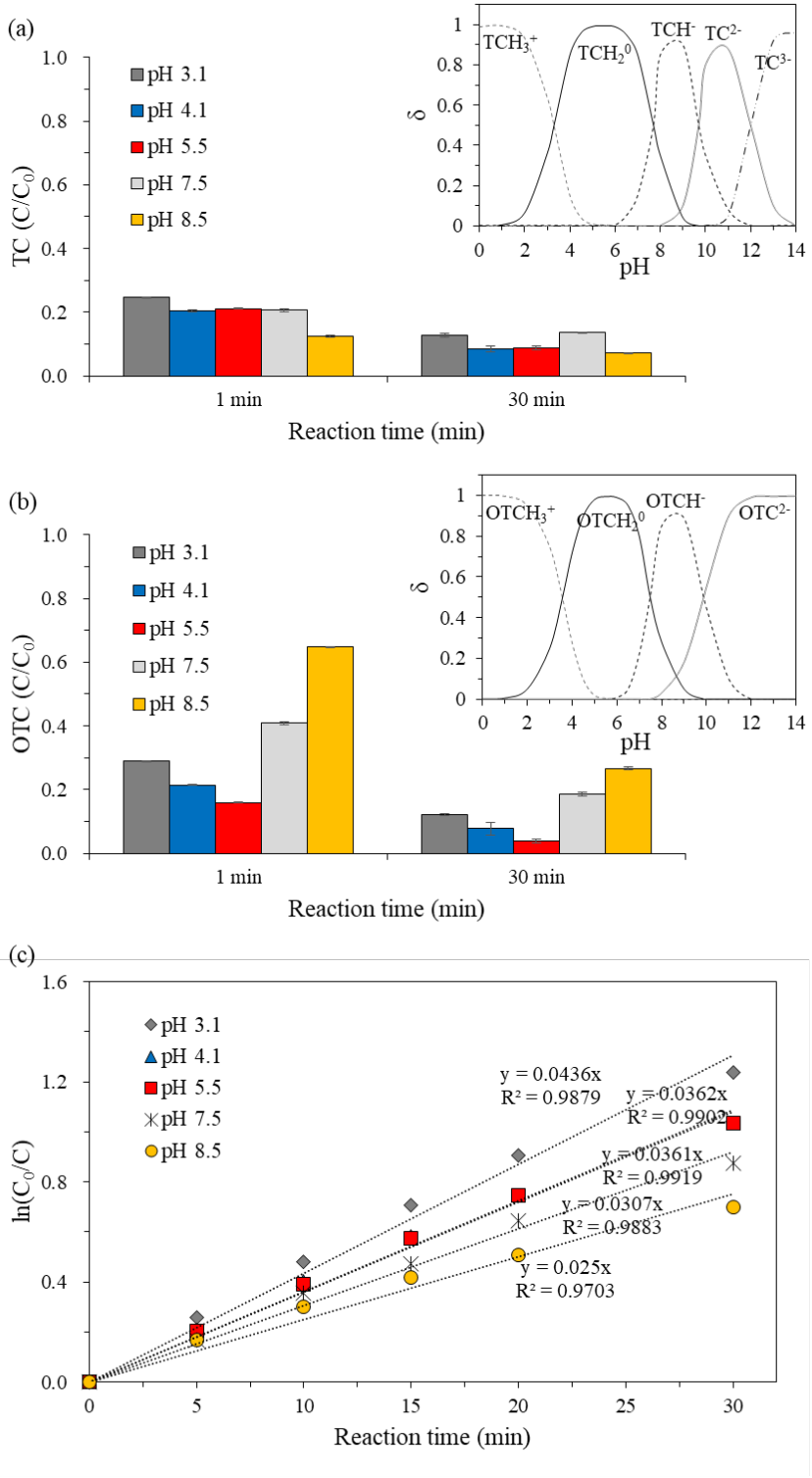
(a)
TC (C/C0)
pH 3.1
pH 4.1
pH 5.5
pH 7.5
pH 8.5
1 min
30 min
Reaction time (min)
δ
pH
TCH3+
TCH20
TCH-
TC2-
TC3-
(b)
OTC (C/C0)
pH 3.1
pH 4.1
pH 5.5
pH 7.5
pH 8.5
1 min
30 min
Reaction time (min)
δ
pH
OTCH3+
OTCH20
OTCH-
OTC2-
(c)
ln(C0/C)
pH 3.1
pH 4.1
pH 5.5
pH 7.5
pH 8.5
y = 0.0436x
R² = 0.9879
y = 0.0362x
R² = 0.9902
y = 0.0361x
R² = 0.9919
y = 0.0307x
R² = 0.9883
y = 0.025x
R² = 0.9703
Reaction time (min)

Fig. 4

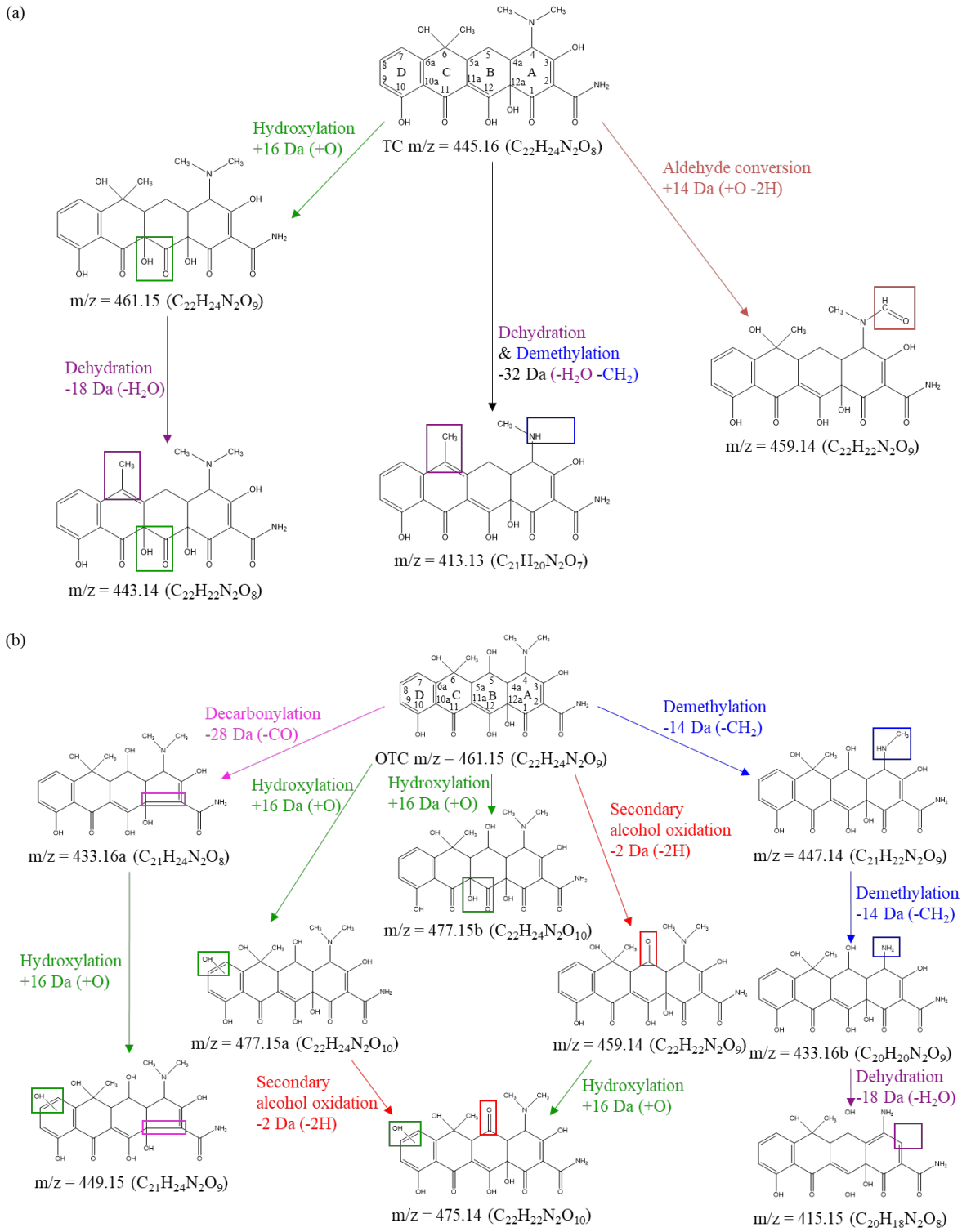
(a)
TC m/z = 445.16 (C22H24N2O8)
Hydroxylation
+16 Da (+O)
Aldehyde conversion
+14 Da (+O -2H)
Dehydration
& Demethylation
-32 Da (-H2O -CH2)
Dehydration
-18 Da (-H2O)
m/z = 461.15 (C22H24N2O9)
m/z = 459.14 (C22H22N2O9)
m/z = 413.13 (C21H20N2O7)
m/z = 443.14 (C22H22N2O8)
(b)
OTC m/z = 461.15 (C22H24N2O9)
Decarbonylation
-28 Da (-CO)
Demethylation
-14 Da (-CH2)
Hydroxylation
+16 Da (+O)
Hydroxylation
+16 Da (+O)
Secondary
alcohol oxidation
-2 Da (-2H)
m/z = 433.16a (C21H24N2O8)
m/z = 447.14 (C21H22N2O9)
m/z = 477.15b (C22H24N2O10)
Demethylation
-14 Da (-CH2)
Hydroxylation
+16 Da (+O)
m/z = 477.15a (C22H24N2O10)
m/z = 459.14 (C22H22N2O9)
m/z = 433.16b (C20H20N2O9)
Secondary
alcohol oxidation
-2 Da (-2H)
Hydroxylation
+16 Da (+O)
Dehydration
-18 Da (-H2O)
m/z = 449.15 (C21H24N2O9)
m/z = 475.14 (C22H22N2O10)
m/z = 415.15 (C20H18N2O8)

Fig. 5

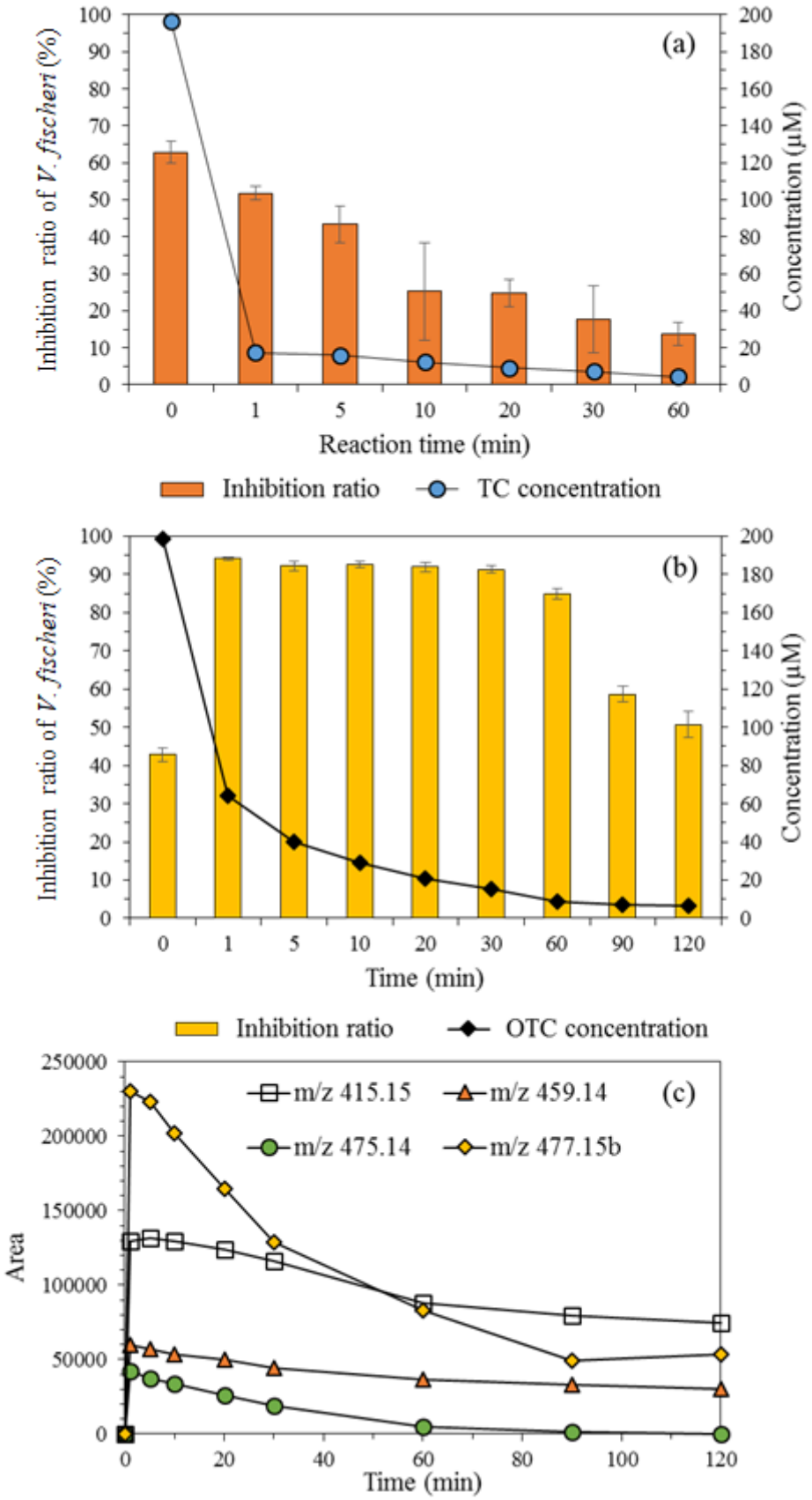
(a)
Inhibition ratio of V. fischeri (%)
Concentration (μM)
Reaction time (min)
Inhibition ratio
TC concentration
(b)
Inhibition ratio of V. fischeri (%)
Concentration (μM)
Time (min)
Inhibition ratio
OTC concentration
(c)
m/z 415.15
m/z 459.14
m/z 475.14
m/z 477.15b
Area
Time (min)

Fig. 6

Table 1

Acute toxicities of OTC and its transformation products determined using the ECOSAR program.

m/z	Fish (LC50, mg/L)	Daphnia (LC50, mg/L)	Green algae (EC50, mg/L)
461.15 (OTC)	1.39×10^5	9435	23848
415.15	5.22×10^6	1.93×10^6	2.43×10^5
459.14	2.93×10^6	1.11×10^6	1.59×10^5
475.14	8.17×10^6	2.98×10^6	3.53×10^5
477.15b	47084	21587	6641